

Phosphorylation of 10-bromoanthracen-9-yl-cyclopenta[*d*]isoxazol-6-ols: chemistry suitable for antivirals

Sarbast M. Ahmed,^a Faiq H. S. Hussain,^b Marco Leusciatti,^c Barbara Mannucci,^d
Mariella Mella,^c and Paolo Quadrelli^{*c}

^aDepartment of Pharmaceutical Chemistry, Pharmacy College
Hawler Medical University, Erbil, Kurdistan Region, Iraq

^bMedical Analysis Department, Faculty of Applied Science
Tishk International University, Erbil, Kurdistan Region, Iraq

^cDepartment of Chemistry, University of Pavia, Viale Taramelli 12, 27100 - Pavia, Italy

^dCentro Grandi Strumenti (CGS), University of Pavia, Via A. Bassi 21, 27100 - Pavia (Italy)

Email: paolo.quadrelli@unipv.it

Received mm-dd-yyyy

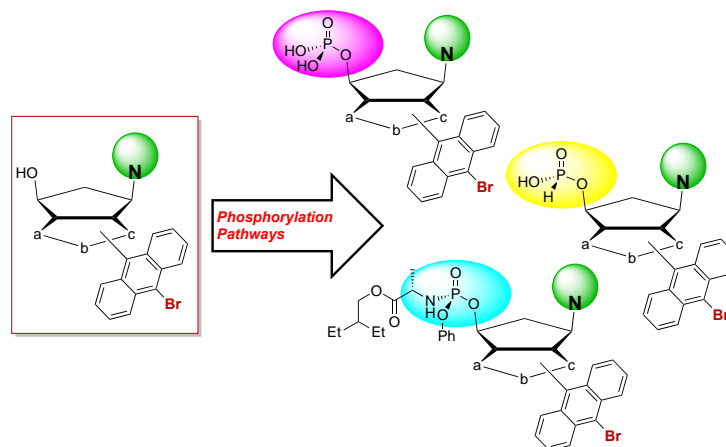
Accepted Manuscript mm-dd-yyyy

Published on line mm-dd-yyyy

Dates to be inserted by editorial office

Abstract

Regioisomeric nor-nucleoside analogues, brominated at the anthracene ring, have been prepared and phosphorylated according to different protocols affording a variety of phosphate and phosphonate derivatives. Chiral phosphorus derivatives were also obtained as inseparable mixtures of diastereoisomers. The synthetic methods are described and found to be reliable and robust, affording nor-nucleosides and nor-nucleotides, available in large amounts for *in vitro* antiviral evaluation.



Keywords: Nor-nucleosides, nor-nucleotides, nitrosocarbonyls, 1,3-dipolar cycloadditions, phosphorylation, antivirals

Introduction

Anthracene and its derivatives represent valuable substituents in biologically active organic molecules. The role of intercalators in DNA between the appropriate base pairs in parallel to their aromatic moieties is clearly suggested by the extended aromatic system characterizing the anthracene ring and its substituted derivatives. In this context, DNA is the main target for the treatment of multiple pathologies, not only cancer.¹ The synthesis of anthracene DNA intercalators is a mature topic in organic chemistry;² nevertheless the presence of the anthracene moiety makes these structures significant, opening up variable strategies for the preparation of innovative derivatives, often characterized by biological activities, in the field of anticancer or antiviral compounds.³ Some isoxazolidinyl polycyclic aromatic hydrocarbons were proposed as DNA-intercalating antitumor agents⁴ and modelling studies⁵ on these structures confirm the degree of binding when a polycyclic aromatic residue is linked to an isoxazoline heterocyclic ring. Several examples can be found in the recent literature on antiviral and anticancer compounds.⁶

Pursuing our investigations on the antiviral behavior of isoxazolino-carbocyclic nor-nucleoside analogues, we synthesized uracil-derivatives that displayed a remarkable antiviral activity with no cellular toxicity at 1-100 μM dose concentration in the case of Human Papilloma virus (HPV).⁷ The binding affinity to the HPV11 E2 protein was evaluated through molecular docking on one of the two regioisomeric structures.

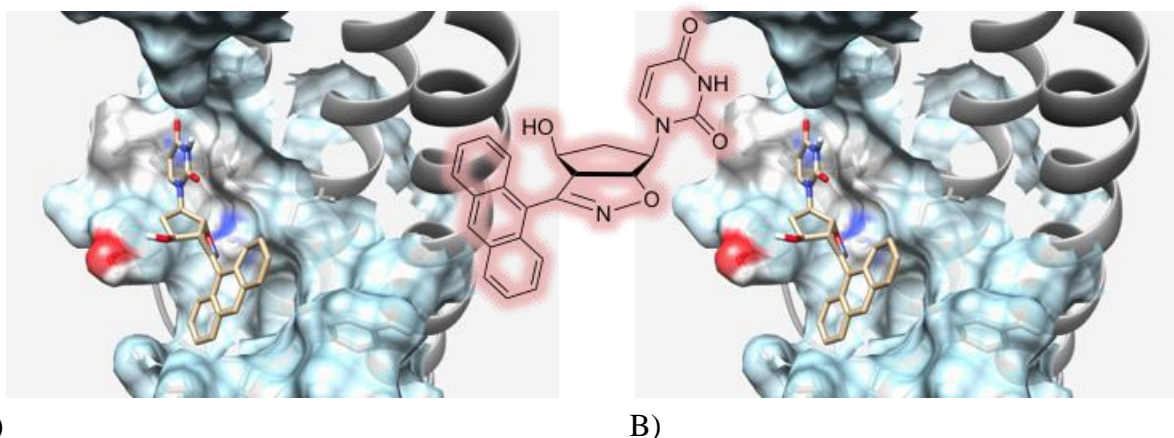


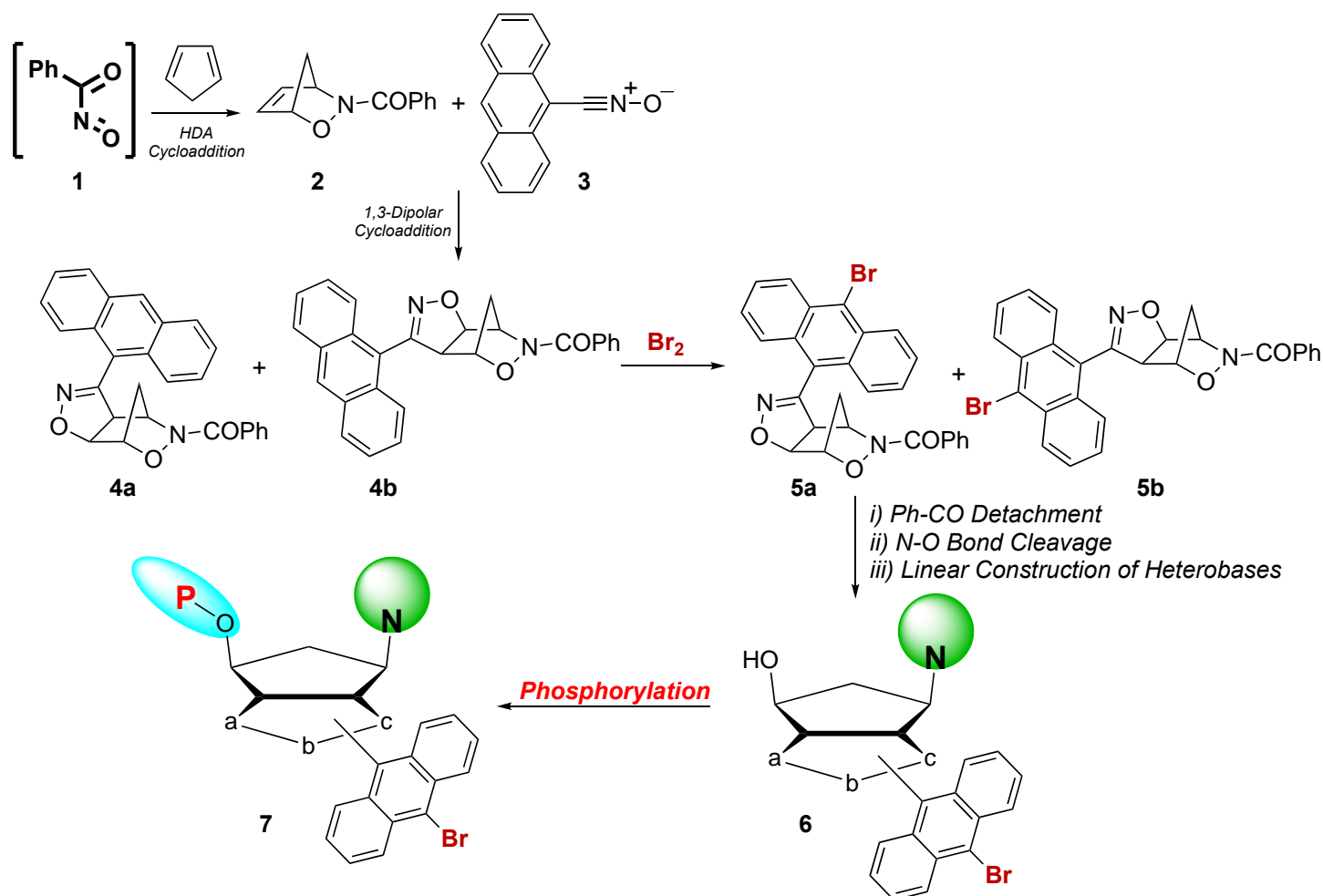
Figure 1. A) Most representative binding mode after 10 ns of molecular dynamic (MD) simulation, starting from the crystal structure of HPV11 E2 protein. B) Binding of the active compound with DNA of HPV-18 from the co-crystallized E2-DNA complex.

As can be seen from Figure 1A, the active compound is anchored at the receptor pocket involved in the protein-protein interaction (PPI) through the isoxazoline ring and the histidine His32 residue. The anthracene and the uracil-substituted cyclopentanol moieties are perfectly complementary to the pocket, and, in particular, the anthracene substituent shades a hydrophobic pocket involved in the specific E2-E1 interaction. A second round of molecular docking calculations was conducted on the specific sequence of DNA recognized by viral E2. We obtained strong indications that the same active compound can specifically bind the DNA minor groove (Figure 1B).

A fine-tuning of the structure of small molecules in structure-activity relationship (SAR) studies can lead to dramatic improvements in the viral inactivation. These tunings can involve the entire structure of candidate molecules or just tiny portions of these molecules, even a single substituent that decorates the structures. Among the groups and molecule portions that can be highlighted in the compounds described in this work, the

anthracene ring attracts attention both for the role cited in the above paragraphs and for the directing ability that this moiety can play in binding modes. From the chemical point of view, anthracene derivatization is seen to be quite easy and fruitful. For example, simple modifications in the structure of the anthracene moiety are often the pivotal step in determining if a compound on the edge of a specific biological activity can collapse to a better or a worse behavior.⁸ Since the C10 carbon atom of the anthracene group is highly reactive and hence a C10-substituent can be easily modified through simple reactions. Thus the introduction of atoms or other functional groups, or even small rings, having variable steric demand, at that position on the anthracene moiety represents an easy way to modify the role of this large polycyclic aromatic ring, orienting the activity towards different biological targets.

Extending of our investigations, we report here the reactions leading from the hetero Diels–Alder (HDA) cycloadduct **2**, prepared from the nitrosocarbonyl intermediate **1** and cyclopentadiene, in the presence of anthracenenitrile oxide **3** (ANO). Bromination processes conducted on the regioisomeric cycloadducts **4a,b** (Scheme 1), afforded the bromo-derivatives **5a,b**. These are the precursors of the target nor-nucleosides of type **6** that are subsequently phosphorylated leading to the compounds **7** in different forms according to the chosen phosphorylation protocol.



Scheme 1. Synthetic strategy towards brominated/phosphorylated nor-nucleotides of type **7**.

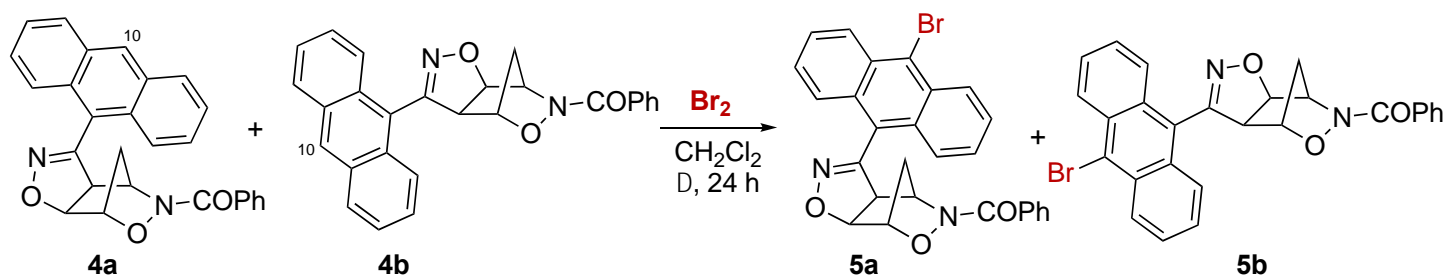
The study aimed to set the experimental conditions of the new synthetic steps introduced in our nucleoside protocol, according to the linear construction of 6-chloro-purine derivatives. First, the bromination reaction introduces selectively a large atom on the anthracene moiety modifying the steric demand of the

polycyclic system at a specific position. In addition, the presence of a bromine offers a means for further functionalizations on the aromatic ring through simple substitution affording suitably designed, more complex derivatives. Secondly, the phosphorylation can be performed according to different protocols aiming to introduce variable phosphorus groups, even chiral, in new nor-nucleotide structures. Thirdly, the choice of the 6-chloropurine ring as heterobase allows for the valuable possibility to further functionalize the heterocyclic ring at the position C6 by replacement of the chlorine atom with various nucleophiles. These reactions can be conducted in a mild and efficient way, thus widening the product family available for different purposes.

Our aim in this proof of concept (POC) study to ascertain the scope and limitations of this chemistry upon variation of the anthracene structure and the phosphorylation methodology, to prepare new compounds with potential antiviral activity.

Results and Discussion

The starting regioisomeric compounds **4a,b** were prepared, according to the published procedure,⁹ from the 2,3-oxazanorborn-5-ene **2** in the presence of a slight excess of anthracenenitrile oxide **3** and isolated in nearly 1:1 ratio by column chromatography (see Scheme 1). The bromination protocol was adapted from the literature procedures¹⁰ and the regioisomeric cycloadducts **4a,b** were converted into the bromo-derivatives **5a,b** upon treatment with bromine under mild conditions (CH₂Cl₂, at reflux for 24 h; Scheme 2).

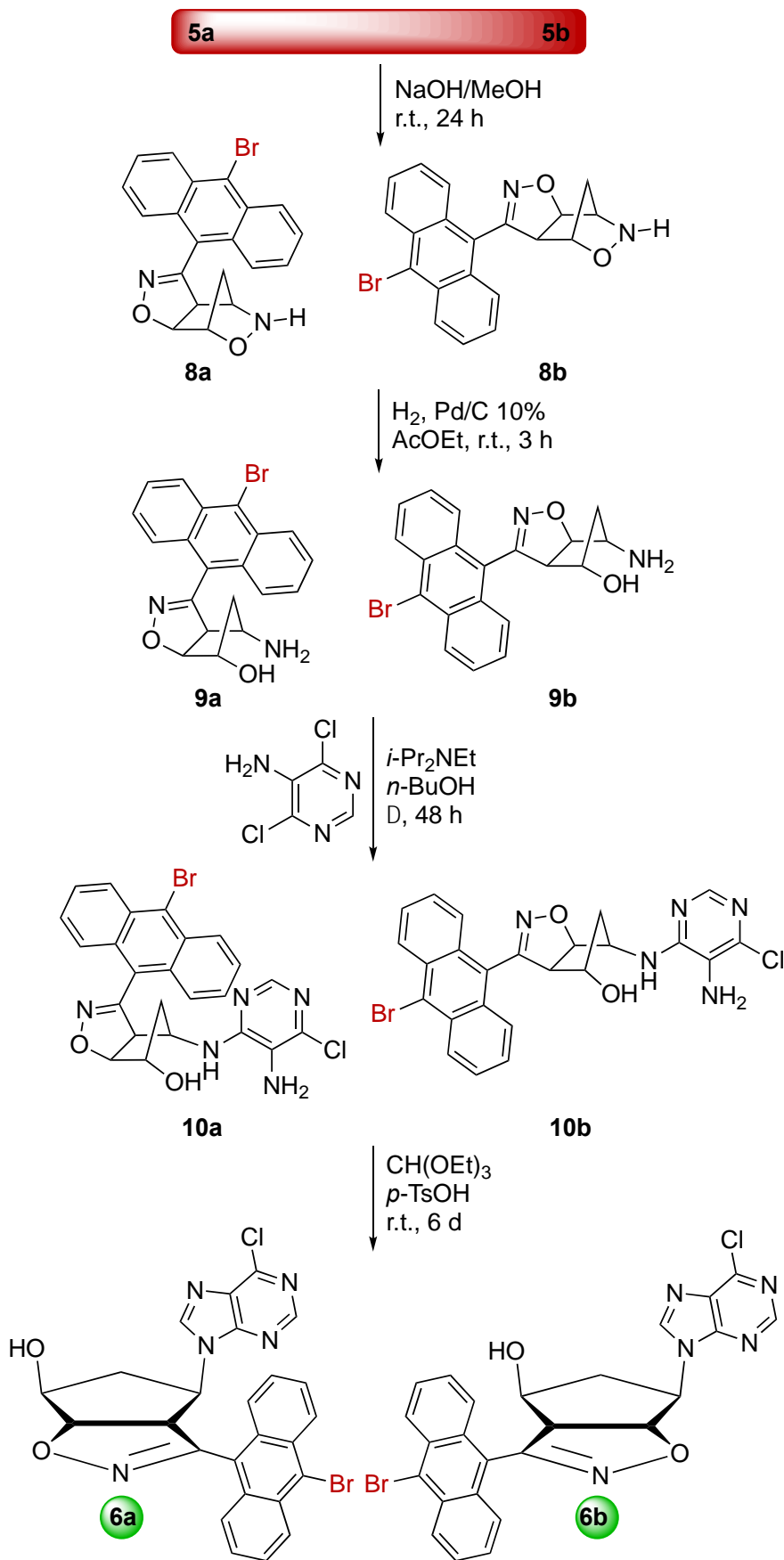


Scheme 2. Bromination of cycloadducts **4a,b**.

Brominated compounds **5a** and **5b** were isolated in excellent yields (95% and 92%, respectively) and were fully characterized. In the ¹H NMR spectra of both compounds **5a,b**, the H10 hydrogen signals, found in the ¹H NMR spectra of **4a** and **4b** at δ 8.62 ppm and δ 8.59 ppm, respectively, were now missing. High resolution mass spectra (HRMS) corroborated the presence in compounds **5a,b** of the bromine atoms, showing the typical isotopic pattern.

The following synthetic steps follow the classical pathway required for the linear construction of purines, as we have shown in previous work,¹¹ with a few adaptations and experimental improvements. The whole synthetic pathways are sketched in Scheme 3.

Alkaline hydrolysis^{7,9} of the cycloadducts **5a,b**, conducted with a solution of powdered NaOH in MeOH, afforded the hydroxylamine derivatives **8a,b** in nearly quantitative yield. The ¹H NMR spectra (DMSO-*d*₆) show the absence of the 5 proton signals corresponding to the benzoyl group, and the presence of signals at δ 6.61 ppm and δ 3.71 ppm, respectively for **8a** and **8b**, corresponding to the NH protons, further attesting to the benzoyl group detachment.



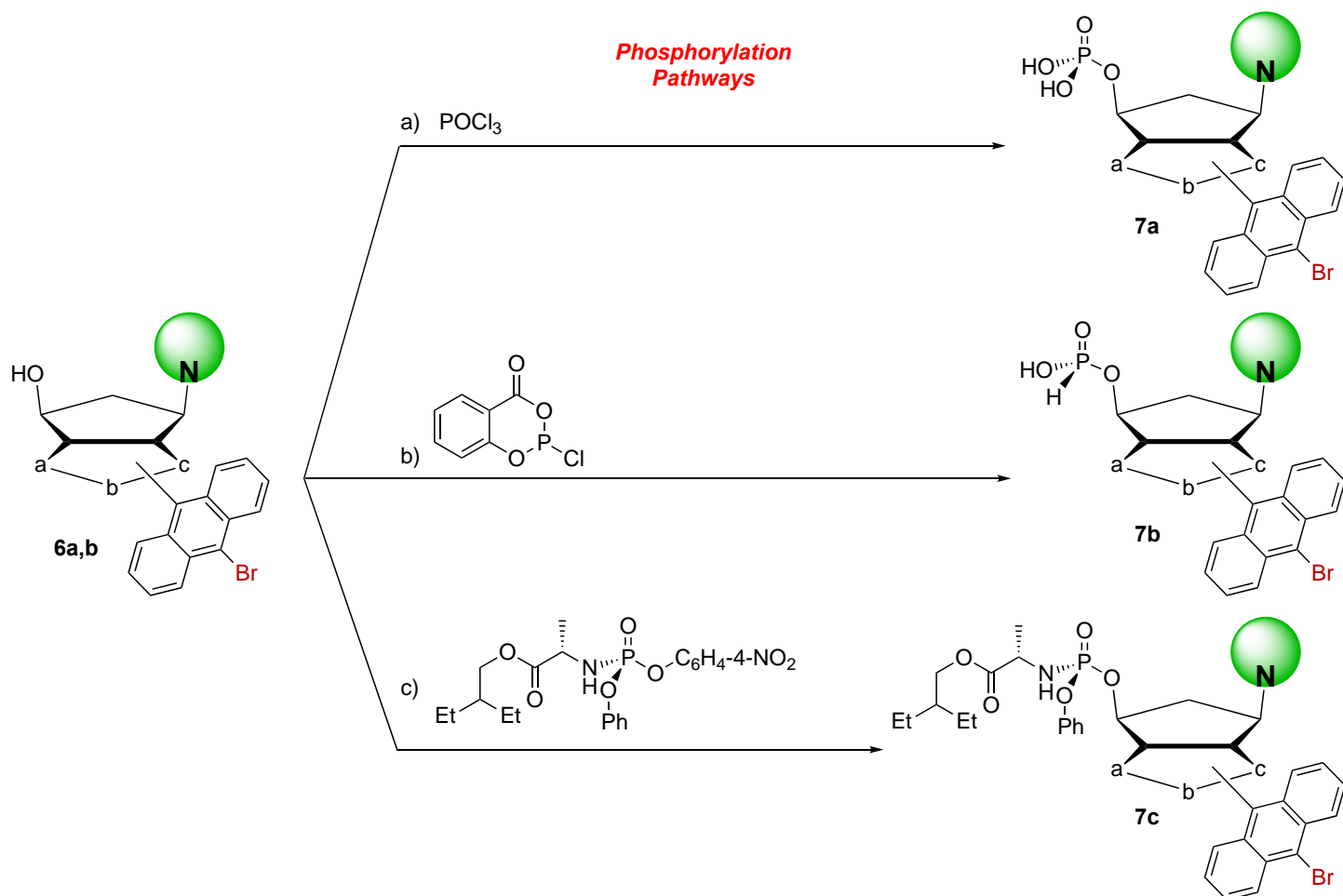
Scheme 3. Synthetic pathway to brominated regioisomeric nor-nucleosides **6a,b**.

Hydrogenolysis^{7,9} of the derivatives **8a,b** under standard conditions (H₂, Pd/C 10%, AcOEt), afforded the desired aminols **9a,b** (yields: 98% and 97%, respectively). The reaction time must be carefully contained within three hours because a prolonged hydrogenation process was detrimental to the stability of the anthracene moiety and a plethora of degradation products was observed in the reaction mixtures. The structures of **9a,b** were confirmed from their analytical and spectroscopic data. In particular, in the ¹H NMR spectra the NH signals had disappeared and the spectrum displayed a more complex fine structure with couplings due to the increased conformational mobility of the cyclopentane moieties following strain relief after the hydrogenolytic ring opening and. Significantly, the NH₂ and OH groups (linked to each other by H-bonding) furnished signals, respectively, at δ 5.94 ppm and δ 8.05 ppm for compound **9a** while for compound **9b** the corresponding groups gave signals at δ 3.32 ppm and δ 8.03 ppm.

By adapting known procedures for the construction of the purine nucleus,^{12,13} the aminols **9a,b** were converted into the pyrimidine derivatives **10a,b** by substitution of 5-amino-4,6-dichloropyrimidine and then into the chloropurines **6a,b** by acid-catalyzed condensation with ethyl orthoformate (Scheme 3). The pyrimidine derivatives **10a,b** were obtained in good yields (**10a**, 56%; **10b**, 66%) in the most delicate synthetic step of the entire pathway, by heating solutions of the aminols **9a,b** and 5-amino-4,6-dichloropyrimidine (2 equiv.) in *n*-BuOH (bp 117 °C) in sealed flasks in the presence of an excess of *i*-Pr₂NEt (5 equiv.) for 48 h. The use of sealed flasks (Schlenk tubes) for these synthetic steps was essential for the success of the reactions since the sealed reactors create a moderate overpressure; control experiments conducted at room pressure resulted in failure of the processes. The structures of **10a,b** rely upon their analytical and spectroscopic data. The IR spectra of pyrimidines **10a,b** exhibit a complex series of bands between 3180-3370 cm⁻¹ due to the presence of OH, NH and NH₂ groups and the ¹H-NMR spectra (DMSO-*d*₆) were unambiguously consistent for the assigned structures where the typical signals corresponding to the pyrimidine moieties (CH=N group) can be found linked to those belonging to the aminol structures.

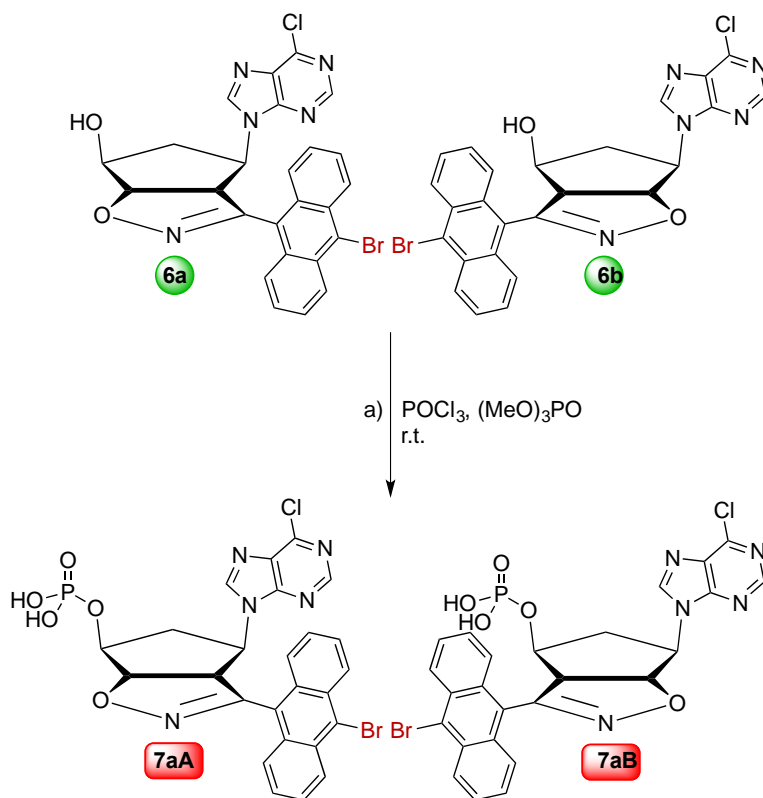
The conversion of the stereoisomeric pyrimidines **10a,b** into the chloropurines **6a,b** was finally achieved in excellent yield (87% for both the products) by treatment with triethyl orthoformate in the presence of catalytic *p*-TsOH, maintaining the reaction mixtures at r.t. for six days and in accordance with a previously reported protocol.¹² Isolation and purification of **6a,b** were secured by hydrolysis of triethyl orthoformate, evaporation of the organic solvent and extraction of the water solution with dichloromethane, followed by crystallization of the final products.

The chloropurines **6a,b** were fully characterized. The infrared spectra of **6a,b** showed a single broad band at 3328 cm⁻¹ (**6a**) and 3413 cm⁻¹ (**6b**) corresponding to the OH absorptions. In the ¹H-NMR spectra (DMSO-*d*₆) the two N=CH protons of the purine rings occur as singlets at δ 8.57 and 8.59 ppm for **6a** and at δ 8.88 and 8.90 ppm for **6b**, these signals being diagnostic of the presence of a purine ring.



Scheme 4. Phosphorylation protocols for the conversion of nor-nucleosides to nor-nucleotide analogues of type **7** as regioisomers.

The conversion of the synthesized nor-nucleosides **6a,b** into nor-nucleotide analogues of type **7a-c** was conducted according to different synthetic approaches with the aim to compare the synthetic methods, finding the best pathway to the desired phosphorus compounds as well as to obtain different types of phosphorus derivatives, even in a diastereoisomeric form. In a POC evaluation, we limited the study to the preparation of monophosphate derivatives, regarding this as the best way to reaching the subsequent goal: the synthesis of triphosphate compounds, essential for the planned *in vitro* antiviral tests to be conducted in collaboration with the biological research group at the University Tor Vergata (Rome). From literature investigations, we found different and valuable methods for the introduction of phosphorus moieties at a different level of complexity and nature.¹⁴ Scheme 4 summarizes the protocols that range from the simple introduction of a phosphate group according to the methods (a) and (b) (hydrolysis is required to furnish the shown functional group)^{15,16} to the method (c) where the introduction of the chiral 2-ethylbutyl (*R*)-(4-nitrophenoxy)(phenoxy)phosphoryl)-L-alaninate¹⁷ allows for the insertion of a phosphorus group, like that in the structure of Remdesivir, one of the compounds recently proposed as an antiviral compound to combat Covid-19.¹⁸ The phosphoryl-L-alaninate is a commercially available residue that can be introduced through nucleophilic substitution, with 4-nitrophenoxide as the leaving group (*vide infra*).

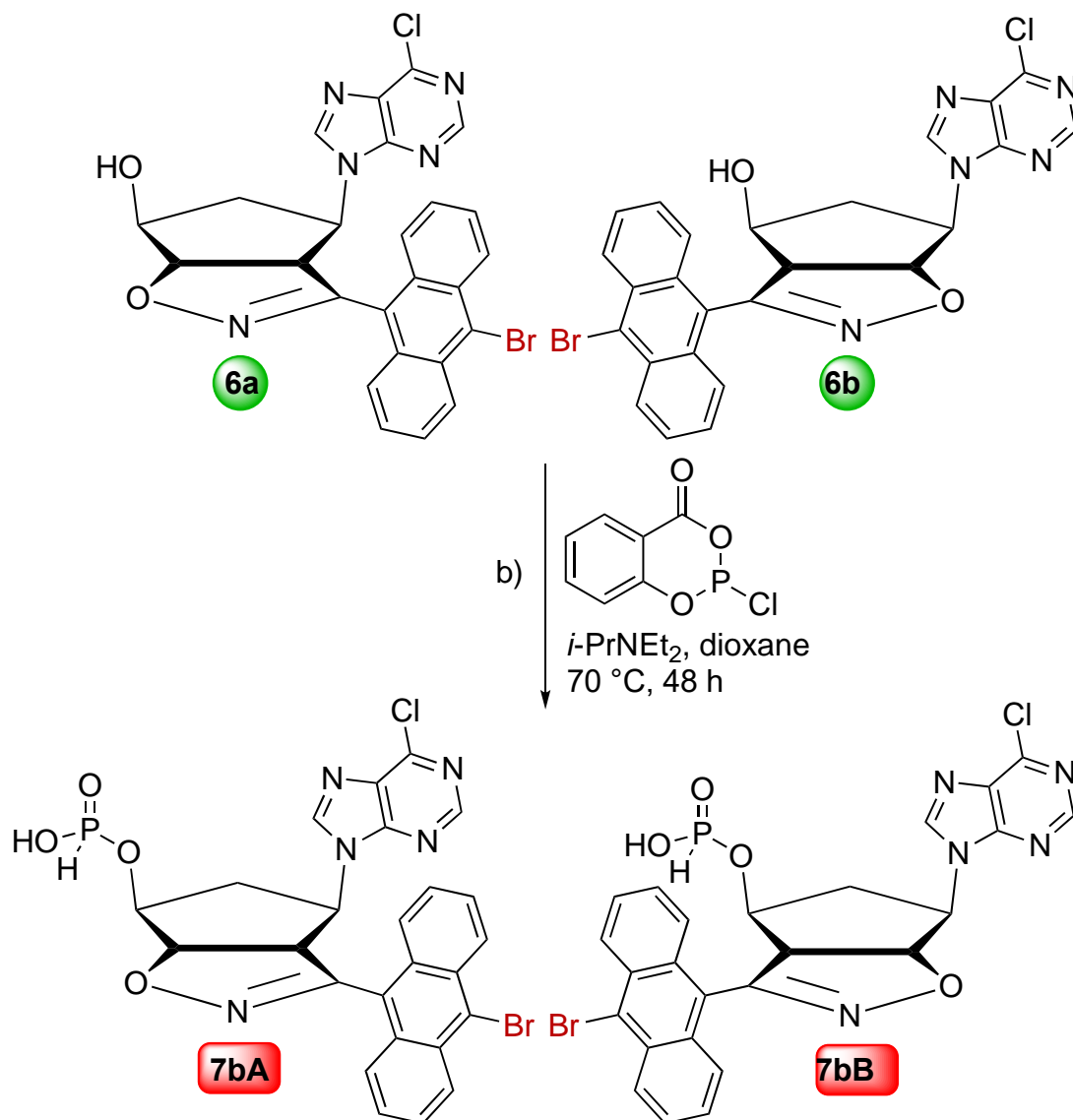


Scheme 5. Synthetic pathways to phosphate derivatives **7a(A,B)**.

We started with the functionalization according to the method (a) aiming to prepare the regioisomeric phosphate derivatives of type **7a**. Treatment of the nor-nucleosides **6a,b** with excess POCl_3 (3 equiv.) in an ice-cooled solution of trimethyl phosphate afforded the desired products **7aA,B** in nearly quantitative yield after an overnight reaction at (Scheme 5). The obtained products were fully characterized spectroscopically. In the ^1H NMR ($\text{DMSO}-d_6$) the structures of the nucleosides were confirmed upon comparison with the spectra of the starting material. Significantly, the absence of the signal relative to the OH group indicates the functionalization with the phosphorus Group. The ^{31}P NMR spectrum ($\text{DMSO}-d_6$) revealed the presence of the phosphate group as a singlet at δ -0.10 ppm for compound **7aA** and at δ -2.10 ppm for compound **7aB**, in full accordance with literature.¹⁹

Alternatively, we investigated the use of the salicylic phosphorus derivative (2-chloro-4H-benzo[d][1,3,2]dioxaphosphinin-4-one) [method (b)] to derivatize the nor-nucleosides **6a,b**. The method led to positive and promising results with the novelty that the products were derivatized as phosphonates of type **7b(A,B)** and were obtained in 78% and 88% yields, respectively (Scheme 6). The protocol was adapted from literature¹⁶ thus the nor-nucleosides **6a,b** were dissolved in anhydrous dioxane and excess $i\text{-Pr}_2\text{NEt}$ along with 1.1 equivalent of the phosphorus reagent. The reactions were conducted in sealed vessels at 70 °C for 48 h, leading to the phosphonate derivatives **7b(A,B)** that were fully characterized.

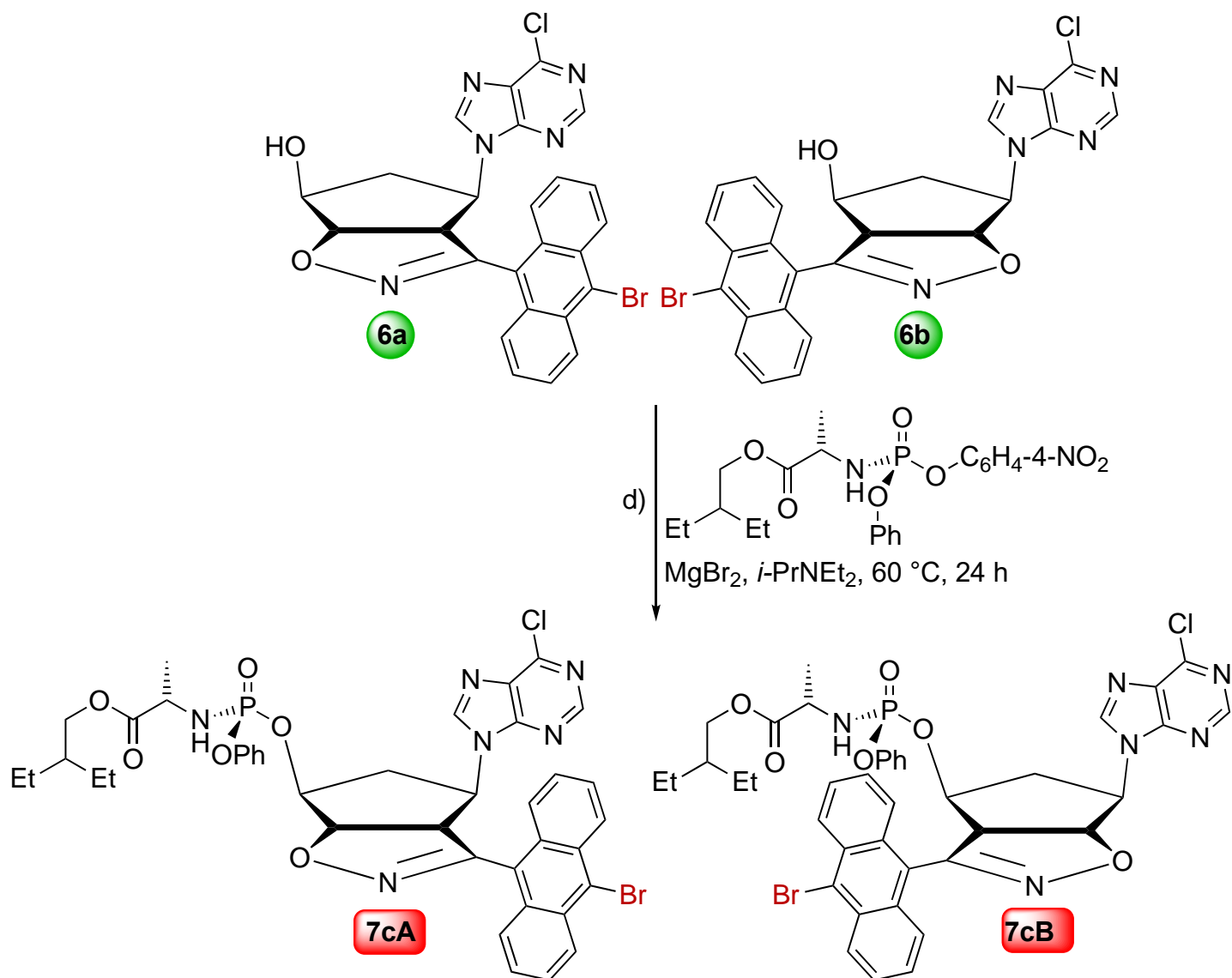
The absence in the ^1H NMR spectra ($\text{DMSO}-d_6$) of the signal relative to the OH proton is due to the presence of the phosphorus group. In particular, ^{31}P NMR spectra demonstrated that the presence of a phosphonate group with a proton directly linked to the phosphorus atom; the ^{31}P signal in the NMR appears at δ 2.20 and 7.70 ppm (d, decoupled δ 5.00 ppm) for compound **7bA** while for compound **7bB** the ^{31}P signal in the NMR appears at δ 0.81 and 4.41 ppm (d, decoupled δ 1.78 ppm). The HRMS spectra corroborated the structures reported in Scheme 6. This method represents the first step for the preparation of triphosphate derivatives.



Scheme 6. Synthesis of phosphonate derivatives **7b(A,B)**.

The 2-ethyl-(*S*)-4-nitrophenoxy-phenoxyphosphoryl-L-alaninate, a chiral moiety that has been used for the derivatization of the Remdesivir nucleoside moiety,¹⁸ has been used to functionalize the nor-nucleosides **6a,b** by adapting the literature procedure in anhydrous acetonitrile in the presence of dry magnesium bromide. Diisopropylethylamine was added subsequently and the reactions were conducted in sealed flasks at 60 °C for 24 h (Scheme 7). Simple crystallization by addition of water to the reaction mixtures and chromatographic purification allowed for obtaining the products **7c(A,B)** in fair yields; the isolated compounds were fully characterized.

The ¹H NMR spectrum of compound **7cA** showed the presence of the newly inserted chiral moiety giving rise to an inseparable mixture of diastereoisomers. In particular the ³¹P NMR spectrum showed the presence of phosphorus group as a singlet. The HRMS spectra confirmed the molecular weight of *m/z* 845.1613 corresponding to the (MW+H). A similar behavior was shown in the characterization of the compound **7cB**, again as mixture of diastereoisomers. To separate these probably needs a different method of separation, perhaps by preparative HPLC on reverse phase.



Scheme 7. Synthesis of the alaninate derivatives **7c(A,B)**.

The phosphorylation processes gave promising, interesting and intriguing results and were pivotal in our strategy oriented to the selection of the best candidate as an antiviral compound and specifically dedicated to the combat the SARS-CoV2 virus or other viral emerging infectious diseases. Regarding this last topic, a first evaluation will be performed through docking computational studies. Although nucleoside/nucleotides analogs, they resemble non-nucleosidic reverse transcriptase inhibitors (NNRTI) that have not yet been found/synthesized to combat SARS-CoV2. In principle, they could recognize allosteric nsp12 sites and interact with sites other than those occupied by Remdesivir. NNRTI are considered potential targets by those molecules inducing little cell death since they should be antiviral and not antitumor candidates.²⁰

Due to the complexity of the structures of the synthesized compounds, in order to verify the maintenance of some typical features that the isoxazoline fused ring produces on the cyclopentane nucleoside spacer (reduced conformational mobility and cyclopentane boat-like conformation),¹² a preliminary conformational analysis was conducted through *ab initio* computational methods at the B3LYP/6-31G* level.²¹ Figure 2 shows the optimized structures of compounds **6a,b** (front and side views) and the corresponding conformers where the 6-chloropurine rings are oriented above the cyclopentane spacer and are indicated as **6a_up** and **6b_up**.

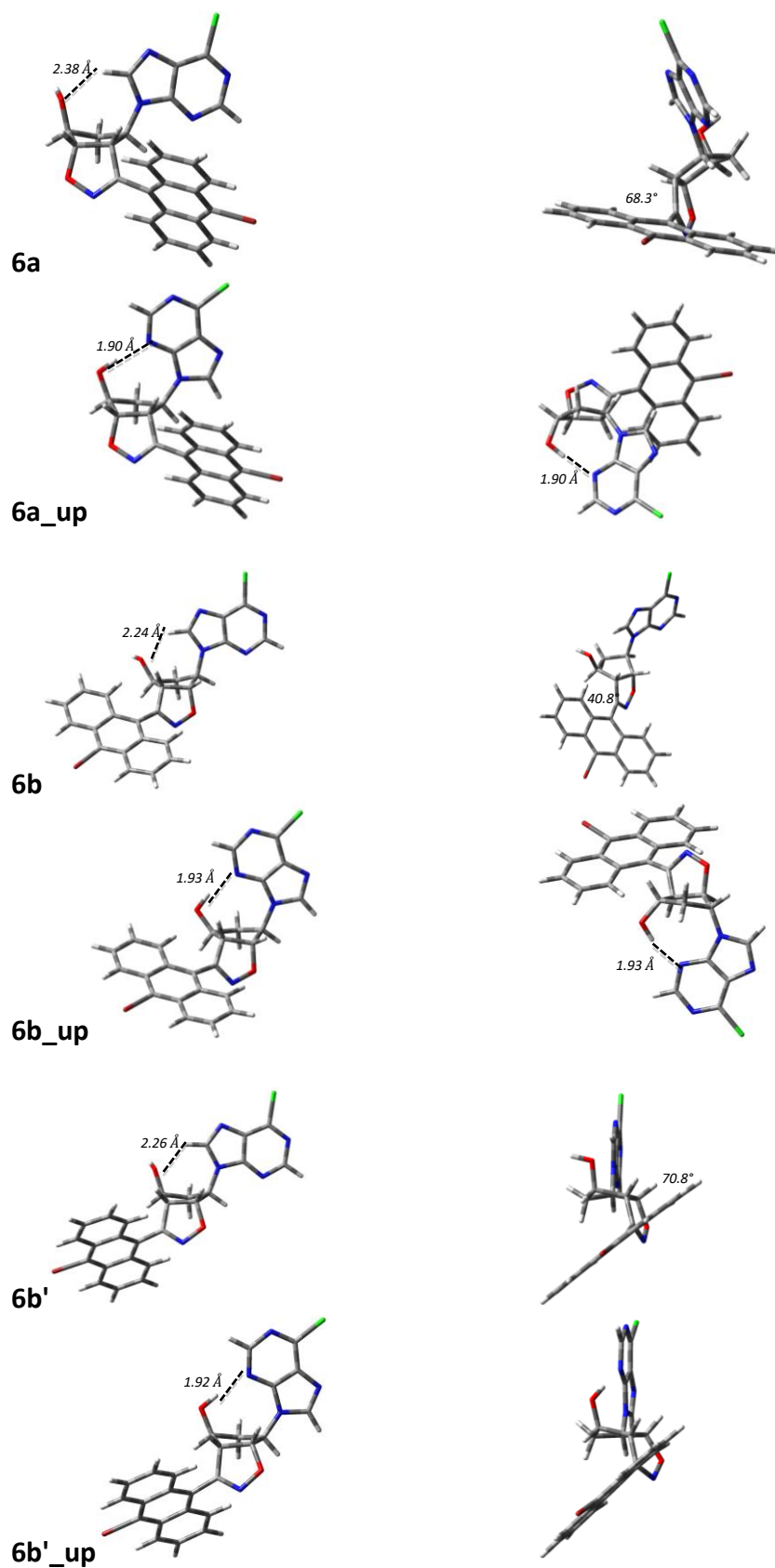


Figure 2. Conformations of nucleosides **6a,b**. Hydrogen-bonding distances are given in Å. Values near the anthracene ring indicate the tilting angles (°).

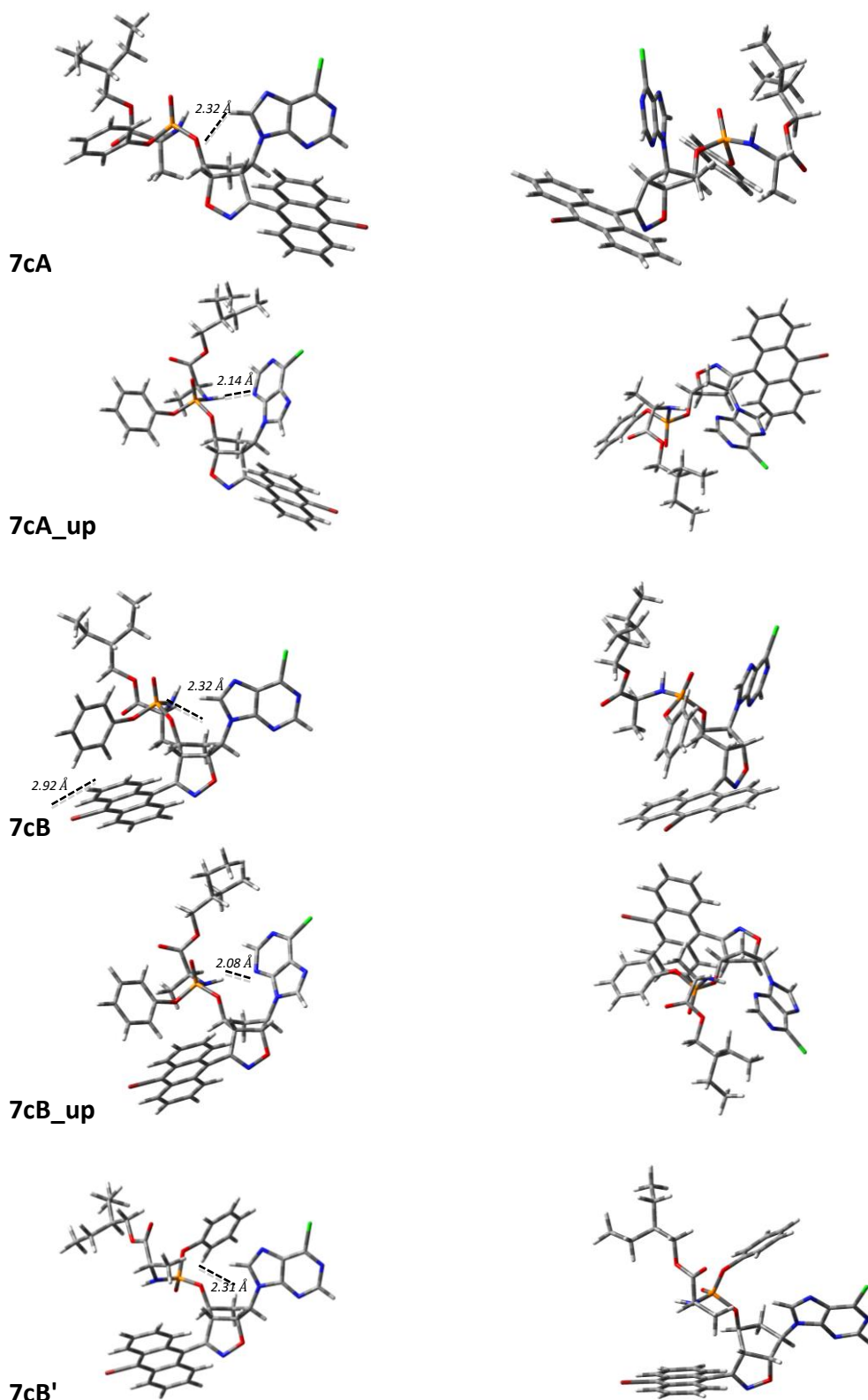


Figure 3. Conformations of nor-nucleosides **7c(A,B)**. Hydrogen-bonding distances are given in Å.

Compounds **6a,b** received a stabilization through an intramolecular hydrogen bond between the CH=N proton of the purine ring (imidazole portion) and the oxygen atom of the secondary alcoholic group (distances are reported in Å in Figure 2). In compound **6a** the anthracene ring is tilted by 68.3° from the conjugation plane with the isoxazoline ring as indicated in Figure 2. The conformer **6a_{up}** gained a larger stabilization (2.27

kcal/mol) from the rotation of the purine ring upward the cyclopentane spacer and a stronger hydrogen bond between the pyrimidine nitrogen atom and the OH alcoholic group located on the spacer.

In both conformations the boat-like appearance of the cyclopentane spacer is conserved, allowing for the relief of non-bonded interactions between the heterocyclic ring and the substituents on the adjacent cyclopentane carbons; the dihedral angles at the five-membered ring range around 90°, thus eliminating the coupling constants in the NMR spectra. The second regioisomeric structure showed two different conformations **6b** and **6b'** where the anthracene moiety is variably oriented. In conformer **6b** the anthracene ring is tilted by an angle of 40.8° inside the isoxazoline-cyclopentane rings with one of the phenyl ring pointing towards the OH group. In conformer **6b'** the anthracene ring is tilted by an angle of 70.8° outside the isoxazoline-cyclopentane rings and this conformer is 8.08 kcal/mol more stable than **6b**. Both these structures showed an intramolecular hydrogen bond between the CH=N proton of the purine ring (imidazole portion) and the oxygen atom of the secondary alcoholic group.

Two other conformers, where the purine ring is rotated up towards the spacer, can be located and labelled **6b_up** and **6b'-up**; these latter were found more stable than the previous described conformers. The intramolecular hydrogen-bonding occurs at shorter distances thus attesting the 2-3 kcal/mol stabilization. Regioisomers of type **b** of the compounds **6** are largely more stable than the **6a** structures reasonably because of the relief of steric effects between the anthracene and purine rings (see Figure 4). Compounds of type **7c(A,B)** showed the same structural features as compounds **6a,b** and for these reasons are not here reported.

We have also optimized the main conformations of the two regioisomeric phosphorylated chiral compounds **7c(A,B)** since they are more complex phosphate derivatives. As we have shown in the previous cases, the nucleoside **7cA** exists in two different conformations, being the second indicated as **7cA_up** more stable by 1.79 kcal/mol because of the hydrogen bonding between the pyrimidine nitrogen atom and the OH alcoholic group located on the spacer (Figure 3).

The regioisomer **7cB** is 2.11 kcal/mol below the isomer **7cA** due to the reasonable relief of steric effects between the anthracene and purine rings. However, the conformer **7cB_up** is even more stable. Conformer **7cB'** differs from the others by the position of the phenoxy group, linked to the phosphorus atom, that is located above the cyclopentane spacer, thus forbidding the purine ring to rotate upward as in the conformations denoted as **_up**. Nevertheless, **7cB'** gains a remarkable stabilization due to the lack of potential repulsive intramolecular interactions.

Figure 4 offers a general view of the relative energies of the optimized conformations for the synthesized compounds of type **6a,b** and **7c**.

This conformational analysis will serve as background to specific computational modeling studies that will assist and validate the design of putative modulators of SARS-CoV2 and other respiratory or emerging viruses, targeting the RNA polymerase, aiming at maximizing the probability of finding active compounds. Part of the computational work will focus on validating and optimizing binding to the active site of RNA polymerase of the newly generated compounds. In parallel, the focus on the main protease with computational drug discovery effort will include the validation of possibly active compounds and their optimization.

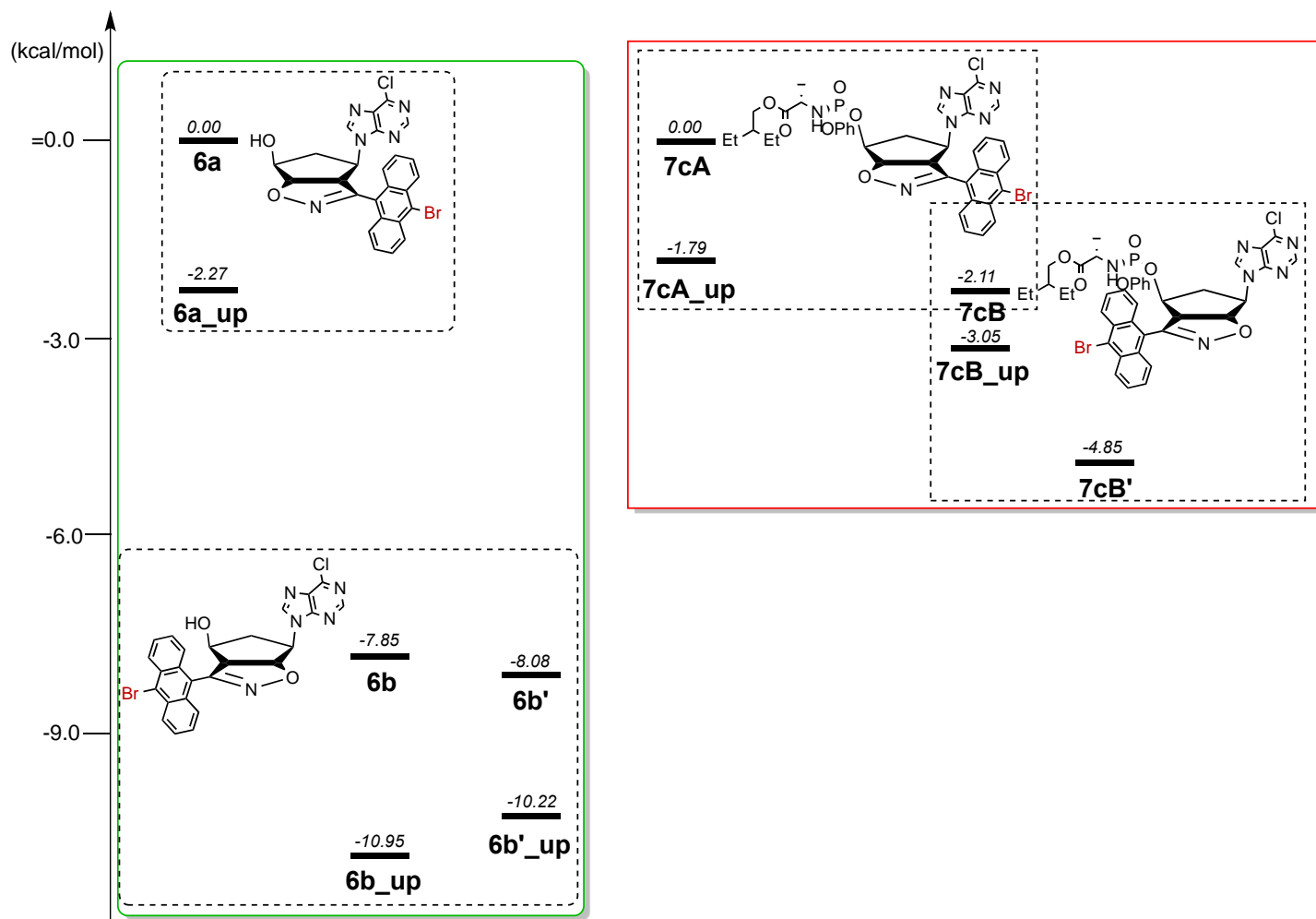


Figure 4. Relative energies (kcal/mol) of optimized conformations for compounds of type **6a,b** and **7c**.

Conclusions

We have synthesized new regioisomeric nor-nucleoside analogues **6a,b**, brominated at the anthracene ring through the linear construction of the purine rings. These nucleosides were phosphorylated according to different methodologies affording a variety of new phosphate and phosphonate derivatives **7**. Chiral phosphorus derivatives were also obtained as inseparable mixtures of diastereoisomers. The carefully adapted synthetic methods were found reliable and robust affording the nor-nucleosides **6a,b** in large amounts. This is an important key point in view of the possibility to functionalize in different ways the structures as mono- or triphosphates by various phosphorylation protocols. The possibility to operate through variable synthetic methodologies as a function of the responses of docking computational experiments will drive the chemical operator to the best structures having the possibility to produce a positive effect in the contrast of viruses' affections.

Among the phosphorylation methods, we set up the experimental conditions to prepare phosphate and phosphonate derivatives through POCl_3 and salicylate phosphorus derivative with reliable protocols nicely applicable to the nor-nucleosides **6a,b** but reasonably also in other cases, without any change/modification in the original structure of compound **6a,b**. This is another pivotal point since the 6-chloropurine moiety is suitable of further derivatization through substitution of the chlorine atom with nucleophiles as shown in

previous works.¹² Nothing of this type happened during the phosphorylation reactions. This type of derivatization at the purine ring will be driven by the computational studies, currently performed in collaboration with a research group at the CNR in Milan. The insertion of the chiral phosphorus group, taken from the structure of Remdesivir, pays tribute to one of the promising molecules that are currently used, in some cases, to combat the pandemic emergency for specific cases. Nevertheless, it seems not to be the definitive solutions and other studies are currently conducted to satisfy the strong demand of molecules other than vaccines to find a complete solution to the health emergency. Our efforts are directed to explore traditional paths introducing the innovation of our reliable chemistry.

Samples of the synthesized compounds have been submitted to the University of Tor Vergata (Rome) for the *in vitro* tests, *in primis* against SARS-CoV2 virus.

Experimental Section

General. All melting points (mp) are uncorrected. ¹H, ¹³C and ³¹P NMR spectra were recorded on a 300 MHz spectrometer (solvents specified). Chemical shifts are expressed in ppm from internal tetramethylsilane (δ) and coupling constants (J) are in Hertz (Hz): b, broad; s, singlet; bs, broad singlet; d, doublet; t, triplet; q, quartet; m, multiplet. IR spectra (nujol mulls) were recorded on a spectrophotometer available at the Department and absorptions (ν) are in cm⁻¹. HRMS measurements were done on a X500B QTOF system (Sciex, Framingham, MA 01701 USA) available at the CGS of the University of Pavia. Column chromatography and tlc: silica gel H60 and GF₂₅₄, respectively; eluants: *c*-C₆H₁₂/EtOAc 9:1 to pure EtOAc.

Compounds **4a,b** were synthesized according to the procedure reported in literature.⁹ Other reagents and solvents were purchased from chemical suppliers and used without any further purification following or adapting the methods reported in the cited literature.

Synthesis of compounds 5a,b through bromination. Compounds **4a,b** (1.5 g, 3.57 mmol) were dissolved in anhydrous CH₂Cl₂ (100 mL) and a bromine solution (0.21 mL, 1.1 equiv.) in CH₂Cl₂ (30 mL) was added dropwise. The reaction was kept in the dark under stirring at reflux for 24 h. Next, the organic phase was washed with an aqueous solution of thiosulfate and dried over anhydrous Na₂SO₄. Upon evaporation of the solvent the crude solid products **5a,b** were collected and recrystallized from EtOH/*i*-Pr₂O and fully characterized.

Compound 5a. 1.69 g (95%), mp 226–228 °C from EtOH/*i*-Pr₂O. IR: ν 1649 (C=O), 1578 (C=N) cm⁻¹. ¹H NMR (300 MHz, DMSO-*d*₆, 25 °C): δ 2.16 and 2.60 (d, 1H+1H, CH₂), 4.37 (d, 1H, *J* 8 Hz, H_{4-isoX}), 4.83 (s, 1H, CH-N), 5.13 (s, 1H, CH-O), 5.37 (d, 1H, *J* 8 Hz, H_{5-isoX}), 7.36 (m, 2H, arom.), 7.48 (m, 1H, arom.), 7.70 (m, 6H, arom.), 8.00 (d, 2H, arom.), 8.68 (d, 2H, arom.). ¹³C NMR (75 MHz, DMSO-*d*₆, 25 °C): δ 33.1, 57.6, 60.6, 80.6, 82.6, 121.6, 124.3, 125.9, 126.9, 127.0, 127.5, 128.4, 128.7, 129.9, 130.1, 131.6, 131.7, 154.2, 171.6. C₂₇H₁₉BrN₂O₃ (499.36): HRMS: calcd. (MW+H) 499.0652; found 499.0647.

Compound 5b. 1.64 g (92%), mp 228–230 °C from EtOH/*i*-Pr₂O. IR: ν 1650 (C=O), 1577 (C=N) cm⁻¹. ¹H NMR (300 MHz, DMSO-*d*₆, 25 °C): δ 2.31 and 2.65 (d, 1H+1H, CH₂), 4.28 (d, 1H, *J* 8 Hz, H_{4-isoX}), 4.54 (s, 1H, CH-N), 5.38 (s, 1H, CH-O), 5.49 (d, 1H, *J* 8 Hz, H_{5-isoX}), 7.45 (m, 2H, arom.), 7.61 (m, 1H, arom.), 7.66 (m, 4H, arom.), 7.77 (d, 2H, arom.), 7.95 (d, 2H, arom.), 8.66 (d, 2H, arom.). ¹³C NMR (75 MHz, DMSO-*d*₆, 25 °C): δ 33.3, 61.6, 62.6, 79.8, 82.5, 122.1, 124.7, 126.2, 127.3, 127.4, 128.2, 128.5, 128.7, 128.8, 130.2, 130.3, 132.0, 154.1, 170.0. C₂₇H₁₉BrN₂O₃ (499.36): HRMS: calcd. (MW+H) 499.0652; found 499.0648.

Synthesis of hydroxylamines (8a,b). Compounds **5a,b** (1.9 g, 3.80 mmol) were dissolved in MeOH (100 mL) and powdered NaOH (0.18 g, 4.50 mmol) was added portionwise at rt. The reaction was left under stirring for 48 h. After this period of time, the solvent was evaporated at reduced pressure and the residue taken up with

CH_2Cl_2 and the organic phase washed with brine and finally dried over anhydrous Na_2SO_4 . Upon evaporation of the solvent the crude solid products **8a,b** were collected and properly recrystallized from EtOAc and fully characterized.

Compound 8a. 1.47 g (98%), mp 180-182 °C from EtOAc. IR: ν 3235 (NH), 1654 (C=N) cm^{-1} . ^1H NMR (300 MHz, $\text{DMSO}-d_6$, 25 °C): δ 1.93 and 2.43 (d, 1H+1H, CH_2), 3.45 (bs, 1H, CH-N), 3.86 (b, 1H, $\text{H}_{4\text{isox.}}$), 4.80 (s, 1H, CH-O), 5.09 (d, 1H, J 8 Hz, $\text{H}_{5\text{isox.}}$), 6.61 (s, 1H, NH), 7.77 (m, 4H, arom.), 8.10 (d, 2H, arom.), 8.56 (d, 2H, arom.). ^{13}C NMR (75 MHz, $\text{DMSO}-d_6$, 25 °C): δ 35.0, 58.3, 61.3, 76.1, 83.7, 123.8, 124.5, 127.2, 127.4, 128.0, 128.7, 154.8. $\text{C}_{20}\text{H}_{15}\text{BrN}_2\text{O}_2$ (395.26): HRMS: calcd. (MW+H) 395.0390; found 395.0396.

Compound 8b. 1.48 g (99%), mp 140-142 °C from EtOAc. IR: ν 3239 (NH), 1624 (C=N) cm^{-1} . ^1H NMR (300 MHz, CDCl_3 , 25 °C): δ 2.19 and 2.71 (d, 1H+1H, CH_2), 3.71 (s, 1H, NH), 4.13 (d, 1H, J 8 Hz, $\text{H}_{4\text{isox.}}$), 3.31 (s, 1H, CH-N), 4.46 (s, 1H, CH-O), 5.42 (d, 1H, J 8 Hz, $\text{H}_{5\text{isox.}}$), 7.67 (m, 4H, arom.), 7.93 (d, 2H, arom.), 8.63 (d, 2H, arom.). ^{13}C NMR (75 MHz, CDCl_3 , 25 °C): δ 34.8, 61.4, 63.0, 77.3, 82.8, 122.3, 124.7, 124.8, 126.0, 127.3, 128.2, 128.6, 130.2, 154.3. $\text{C}_{20}\text{H}_{15}\text{BrN}_2\text{O}_2$ (395.26): HRMS: calcd. (MW+H) 395.0390; found 395.0392.

Synthesis of aminols (9a,b). Compounds **8a,b** (1.4 g, 3.54 mmol) were dissolved in EtOAc (70 mL) along with 0.4 g C/Pd 10% and the mixture was submitted to hydrogenation at rt. The reaction was left under stirring with hydrogen stream for 3 h. After this period of time, the solution was filtered and the solvent was evaporated to dryness. The crude solid products **9a,b** were recrystallized from *i*-Pr₂O and fully characterized.

Compound 9a. 1.38 g (98%), mp 75-78 °C from *i*-Pr₂O. IR: ν 3348, 3284 (NH₂), 3176 (OH), 1622 (C=N) cm^{-1} . ^1H NMR (300 MHz, $\text{DMSO}-d_6$, 25 °C): δ 1.93 and 2.25 (m, 1H+1H, CH_2), 3.22 (m, 1H, CH-N), 4.41 (m, 1H, $\text{H}_{4\text{isox.}}$), 4.48 (m, 1H, CH-O), 5.42 (m, 1H, $\text{H}_{5\text{isox.}}$), 5.94 (bs, 2H, NH₂), 7.64 (m, 4H, arom.), 8.05 (bs, 1H, OH), 8.21 (d, 2H, arom.), 8.57 (d, 2H, arom.). ^{13}C NMR (75 MHz, $\text{DMSO}-d_6$, 25 °C): δ 37.2, 59.7, 63.5, 76.5, 91.3, 106.8, 122.3, 125.5, 125.6, 127.3, 127.7, 128.2, 128.9, 129.1, 129.6, 130.8, 154.7. $\text{C}_{20}\text{H}_{17}\text{BrN}_2\text{O}_2$ (397.27): HRMS: calcd. (MW+H) 397.0546; found 397.0533.

Compound 9b. 1.37 g (97%), mp 78-80 °C from *i*-Pr₂O. IR: ν 3366, 3303 (NH₂), 3180 (OH), 1654 (C=N) cm^{-1} . ^1H NMR (300 MHz, $\text{DMSO}-d_6$, 25 °C): δ 1.71 and 2.11 (m, 1H+1H, CH_2), 3.32 (bs, 2H, NH₂), 3.63 (m, 1H, CH-N), 3.83 (m, 1H, CH-O), 4.28 (d, 1H, J 8 Hz, $\text{H}_{4\text{isox.}}$), 5.29 (d, 1H, J 8 Hz, $\text{H}_{5\text{isox.}}$), 7.61 (m, 4H, arom.), 8.03 (d, 1H, J 4 Hz, OH), 7.96 (d, 2H, arom.), 8.19 (d, 2H, arom.). ^{13}C NMR (75 MHz, $\text{DMSO}-d_6$, 25 °C): δ 39.8, 59.5, 67.1, 74.9, 92.9, 123.1, 124.7, 125.6, 127.1, 127.6, 128.2, 128.7, 129.1, 129.6, 130.8, 154.9. $\text{C}_{20}\text{H}_{17}\text{BrN}_2\text{O}_2$ (397.27): HRMS: calcd. (MW+H) 397.0546; found 397.0531.

Synthesis of pyrimidine derivatives (10a,b). Compounds **9a,b** (1.9 g, 4.78 mmol) were dissolved in *n*-BuOH (40 mL) and 5-amino-4,6-dichloropyrimidine (1.57 g, 9.57 mmol) were added to the solution along with excess *i*-Pr₂NEt (3.09 g, 23.91 mmol). The mixtures were heated at 117 °C in a sealed flask for 48 h. After this period of time, the reactions were quenched with brine and extracted with CH_2Cl_2 (2 x 15 mL) and the organic phases dried over anhydrous Na_2SO_4 . Upon evaporation of the solvent, the residues were submitted to chromatographic purification to isolate the crude solid products **10a,b** that were recrystallized from EtOH/*i*-Pr₂O and fully characterized.

Compound 10a. 1.40 g (56%), mp 246-248 °C from EtOH/*i*-Pr₂O. IR: ν 3362, 3320 (NH₂), 3180 (OH), 1571 (C=N) cm^{-1} . ^1H NMR (300 MHz, $\text{DMSO}-d_6$, 25 °C): δ 1.99 and 2.28 (m, 1H+1H, CH_2), 4.08 (m, 1H, CH-N), 4.41 (m, 1H, $\text{H}_{4\text{isox.}}$), 4.51 (m, 1H, CH-O), 4.85 (s, 2H, NH₂), 5.33 (m, 1H, $\text{H}_{5\text{isox.}}$), 5.50 (d, 1H, J 4 Hz, OH), 6.46 (d, 1H, J 7 Hz, NH), 7.60 (m, 4H, arom.), 8.09 (d, 2H, arom.), 8.20 (d, 2H, arom.), 8.77 (s, 1H, CH=N). ^{13}C NMR (75 MHz, $\text{DMSO}-d_6$, 25 °C): δ 30.7, 55.1, 64.0, 76.8, 91.6, 123.4, 124.8, 125.8, 126.9, 127.3, 127.5, 128.0, 128.7, 129.5, 130.8, 136.8, 144.1, 150.3, 155.8. $\text{C}_{24}\text{H}_{19}\text{BrClN}_5\text{O}_2$ (524.80): HRMS: calcd. (MW-H) 522.0338; found 522.0322.

Compound 10b. 1.66 g (66%), mp 116-118 °C from

EtOH/*i*-Pr₂O. IR: ν 3373, 3327 (NH₂), 3181 (OH), 1570 (C=N) cm⁻¹. ¹H NMR (300 MHz, DMSO-*d*₆, 25 °C): δ 1.91 and 2.39 (m, 1H+1H, CH₂), 4.02 (m, 1H, CH-N), 4.33 (d, 1H, *J* 8 Hz, H₄_{isox.}), 4.78 (m, 1H, CH-O), 5.04 (s, 2H, NH₂), 5.13 (d, 1H, *J* 4 Hz, OH), 5.50 (d, 1H, *J* 8 Hz, H₅_{isox.}), 6.71 (d, 1H, *J* 7 Hz, NH), 7.66 (m, 4H, arom.), 8.02 (d, 2H, arom.), 8.21 (d, 2H, arom.), 8.81 (s, 1H, CH=N). ¹³C NMR (75 MHz, DMSO-*d*₆, 25 °C): δ 30.7, 58.7, 66.7, 73.9, 89.7, 122.8, 123.7, 124.3, 124.8, 125.7, 127.2, 127.6, 128.8, 130.8, 137.9, 146.1, 151.7, 155.3. C₂₄H₁₉BrClN₅O₂ (524.80): HRMS: calcd. (MW-H) 522.0338; found 522.0325.

Synthesis of nucleosides (6a,b). Pyrimidine derivatives **10a,b** (1.0 g, 1.91 mmol) were dissolved in triethyl orthoformate (50 mL) and the solution stirred for a couple of hours. After this period of time, a catalytic amount of *p*-TsOH was added and the solutions left at rt for 6 days. The reactions were quenched with H₂O and extracted with CH₂Cl₂ (2 x 20 mL) and the organic phases dried over anhydrous Na₂SO₄. Upon evaporation of the solvent, the solid crude products **6a,b** were recrystallized from EtOH/*i*-Pr₂O and fully characterized.

Compound 6a. 0.68 g (67%), mp 183-185 °C from EtOH/*i*-Pr₂O. IR: ν 3328 (OH), 1589 (C=N) cm⁻¹. ¹H NMR (300 MHz, DMSO-*d*₆, 25 °C): δ 2.40 and 2.59 (m, 1H+1H, CH₂), 4.61 (bs, 1H, CH-N), 4.78 (m, 1H, CH-O), 5.10 (d, 1H, *J* 8 Hz, H₄_{isox.}), 5.54 (d, 1H, *J* 8 Hz, H₅_{isox.}), 5.71 (b, 1H, OH), 7.71 (m, 4H, arom.), 8.15 (m, 4H, arom.), 8.57 (s, 1H, CH=N), 8.59 (s, 1H, CH=N). ¹³C NMR (75 MHz, DMSO-*d*₆, 25 °C): δ 37.8, 57.2, 63.3, 76.6, 92.2, 123.1, 124.5, 125.4, 125.6, 127.6, 127.7, 128.0, 128.8, 129.5, 130.7, 146.1, 150.3, 150.6, 154.2. C₂₅H₁₇BrClN₅O₂ (534.80): HRMS: calcd. (MW+FA-H) 578.0236; found 578.0238.

Compound 6b. 0.79 g (77%), mp 202-204 °C from EtOH/*i*-Pr₂O. IR: ν 3413 (OH), 1558 (C=N) cm⁻¹. ¹H NMR (300 MHz, DMSO-*d*₆, 25 °C): δ 2.50 and 2.68 (m, 1H+1H, CH₂), 4.16 (bs, 1H, CH-N), 4.56 (d, 1H, *J* 8 Hz, H₄_{isox.}), 5.29 (bs, 1H, OH), 5.48 (bs, 1H, CH-O), 6.04 (dd, 1H, *J* 8, 2 Hz, H₅_{isox.}), 7.79 (m, 4H, arom.), 8.16 (m, 2H, arom.), 8.59 (d, 2H, arom.), 8.87 (s, 1H, CH=N), 8.90 (s, 1H, CH=N). ¹³C NMR (75 MHz, DMSO-*d*₆, 25 °C): δ 38.2, 61.7, 67.2, 72.9, 89.3, 123.6, 124.5, 125.7, 127.7, 128.3, 129.6, 130.4, 131.2, 146.7, 149.1, 151.5, 151.9, 155.4. C₂₅H₁₇BrClN₅O₂ (534.80): HRMS: calcd. (MW+FA-H) 578.0236; found 578.0229.

Synthesis of nucleotides analogues 7aA and 7aB. To an ice-cooled solution of POCl₃ (0.45 mmol) in trimethyl phosphate (0.50 mL), nucleosides **6a** or **6b** (80 mg, 0.15 mmol) were added and the solutions were left under stirring at rt overnight. The reactions were then diluted with Et₂O (50 mL) and H₂O was added (50 mL); upon shaking a solid precipitates and is furtherly collected by filtration under vacuum. The solid crude products **7aA** and **7aB** were recrystallized from EtOH/H₂O and fully characterized.

Compound 7aA. 80.2 mg (87%), mp 220 °C (dec.) from EtOH/H₂O. IR: ν 3245 (OH), 1582 (C=N) cm⁻¹. ¹H NMR (300 MHz, DMSO-*d*₆, 25 °C): δ 2.40 and 2.57 (m, 1H+1H, CH₂), 4.61 (bs, 1H, CH-N), 4.79 (m, 1H, CH-O), 5.10 (d, 1H, *J* 8 Hz, H₄_{isox.}), 5.54 (d, 1H, *J* 8 Hz, H₅_{isox.}), 7.75 (m, 4H, arom.), 8.15 (m, 4H, arom.), 8.57 (s, 1H, CH=N), 8.77 (s, 1H, CH=N). ¹³C NMR (75 MHz, DMSO-*d*₆, 25 °C): δ 37.8, 57.2, 63.3, 76.6, 92.2, 123.1, 124.5, 124.7, 125.4, 125.6, 127.3, 127.6, 128.1, 128.8, 129.3, 129.5, 130.5, 130.7, 146.1, 148.4, 150.3, 151.0, 154.2. ³¹P NMR (121.5 MHz, DMSO-*d*₆, 25 °C): δ -0.10 [s, -PO(OH)₂]. C₂₅H₁₈BrClN₅O₅P (614.78): HRMS: calcd. (MW-H) 611.9845; found 611.9836.

Compound 7aB. 89.5 mg (97%), mp >250 °C (dec.) from EtOH/H₂O. IR: ν 3265 (OH), 1582 (C=N) cm⁻¹. ¹H NMR (300 MHz, DMSO-*d*₆, 25 °C): δ 2.46 and 2.68 (m, 1H+1H, CH₂), 4.15 (bs, 1H, CH-N), 4.56 (d, 1H, *J* 8 Hz, H₄_{isox.}), 5.48 (bs, 1H, CH-O), 6.04 (dd, 1H, *J* 8, 2 Hz, H₅_{isox.}), 7.81 (m, 4H, arom.), 8.15 (m, 2H, arom.), 8.59 (d, 2H, arom.), 8.88 (s, 1H, CH=N), 8.90 (s, 1H, CH=N). ¹³C NMR (75 MHz, DMSO-*d*₆, 25 °C): δ 38.2, 61.7, 67.2, 72.9, 89.3, 123.6, 124.6, 125.7, 127.3, 127.7, 128.3, 128.9, 129.1, 130.8, 131.1, 146.7, 151.6, 151.9, 155.4. ³¹P NMR (121.5 MHz, DMSO-*d*₆, 25 °C): δ -2.10 [s, -PO(OH)₂]. C₂₅H₁₈BrClN₅O₅P (614.78): HRMS: calcd. (MW-H) 611.9845; found 611.9836.

Synthesis of nucleotides 7b(A,B). Nucleosides **6a,b** (150 mg, 0.28 mmol) were dissolved in anhydrous dioxane (5 mL) and excess *i*-Pr₂NH (0.07 mL, 0.42 mmol) was added along with salicyl chlorophosphite (63 mg, 0.31

mmol). The reactions were conducted in a sealed flask under vigorous stirring at 70 °C for 48 h. The reactions were quenched by adding H₂O (50 mL); upon shaking a solid precipitates and is furtherly collected by filtration under vacuum. The solid crude products **7b(A,B)** were recrystallized from EtOH/H₂O and fully characterized.

Compound 7bA. 134.3 mg (78%), mp 238 °C (dec.) from EtOH/H₂O. IR: ν 3393 (OH), 1586 (C=N) cm⁻¹. ¹H NMR (300 MHz, DMSO-*d*₆, 25 °C): δ 2.40 and 2.67 (m, 1H+1H, CH₂), 4.61 (bs, 1H, CH-N), 4.79 (m, 1H, CH-O), 5.09 (d, 1H, *J* 8 Hz, H4_{isox.}), 5.54 (d, 1H, *J* 8 Hz, H5_{isox.}), 7.71 (m, 4H, arom.), 8.15 (m, 4H, arom.), 8.53 (s, 1H, CH=N), 8.59 (s, 1H, CH=N). ¹³C NMR (75 MHz, DMSO-*d*₆, 25 °C): δ 38.2, 57.6, 63.6, 76.9, 92.6, 123.5, 124.9, 125.1, 125.8, 126.0, 127.9, 128.1, 128.4, 129.2, 129.9, 130.9, 131.1, 146.5, 150.7, 151.4, 154.6. ³¹P NMR (121.5 MHz, DMSO-*d*₆, 25 °C): δ 2.20 and 7.70 [d, *J* 668 Hz, -P(O)(H)OH]; decoupled: δ 5.00 [s, -P(O)(H)OH]. C₂₅H₁₈BrClN₅O₄P (598.78): HRMS: calcd. (MW-H) 595.9896; found 595.9887.

Compound 7bB. 151.5 mg (88%), mp 160-162 °C (dec.) from EtOH/H₂O. IR: ν 3411 (OH), 1588 (C=N) cm⁻¹. ¹H NMR (300 MHz, DMSO-*d*₆, 25 °C): δ 2.67 and 2.80 (m, 1H+1H, CH₂), 3.37 (m, 1H, OH), 4.61 (m, 1H, CH-N), 4.84 (d, 1H, *J* 8 Hz, H4_{isox.}), 5.53 (bs, 1H, CH-O), 6.10 (d, 1H, *J* 8 Hz, H5_{isox.}), 7.78 (m, 3H, arom.), 8.16 (m, 3H, arom.), 8.56 (d, 2H, arom.), 8.87 (s, 1H, CH=N), 8.89 (s, 1H, CH=N). ¹³C NMR (75 MHz, DMSO-*d*₆, 25 °C): δ 39.0, 53.1, 61.4, 74.9, 89.0, 122.9, 124.7, 124.8, 125.6, 125.7, 127.4, 128.2, 128.9, 129.5, 130.4, 130.7, 131.1, 146.4, 149.1, 151.6, 154.5. ³¹P NMR (121.5 MHz, DMSO-*d*₆, 25 °C): δ 0.81 and 4.41 [d, *J* 347 Hz, -P(O)(H)OH]; decoupled: δ 1.78 [s, -P(O)(H)OH]. C₂₅H₁₈BrClN₅O₄P (598.78): HRMS: calcd. (MW-H) 595.9896; found 595.9877.

Synthesis of nucleotides 7c(A,B). Nucleosides **6a,b** (150 mg, 0.28 mmol) were dissolved in anhydrous acetonitrile (20 mL) along with 2-ethyl-(*S*)-4-nitrophenoxy-phenoxyphosphoryl-L-alaninate (152 mg, 0.34 mmol), dry magnesium bromide (52 mg, 0.28 mmol) and *i*-Pr₂NEt (2.5 equiv.). The mixtures were heated in sealed flasks at 60 °C for 24 h. After this period of time, the mixtures were then diluted with H₂O and extracted with EtOAc (2 x 50 mL) and the organic phases dried over anhydrous sodium sulfate. Simple addition of H₂O to the reaction mixtures can promote crystallization of solid products that can be filtered and purified either by recrystallization or through column chromatography. Products **7c(A,B)** were then fully characterized.

Compound 7cA. 40 mg (16%), semi-solid compound. IR: ν 1733 (C=O), 1584 (C=N) cm⁻¹. ¹H NMR (300 MHz, DMSO-*d*₆, 25 °C): δ 0.83 (t, 3H, *J* 7 Hz, CH₃), 1.29 (m, 4H+3H, CH₃ and CH₂), 1.42 (m, 1H, CH), 2.75 and 2.86 (m, 1H+1H, CH₂), 3.95 (m, 2H, CH₂-O), 4.84 (bs, 1H, CH-N), 5.29 (m, 1H+1H, CH-O and H4_{isox.}), 5.82 (d, 1H, *J* 8 Hz, H5_{isox.}), 6.19 (m, 1H, NH), 7.18 (m, 2H, arom.), 7.31 (m, 2H, arom.), 7.61 (m, 1H, arom.), 7.75 (m, 4H, arom.), 8.10 (m, 3H, arom.), 8.48 (m, 1H+1H, arom. and CH=N), 8.53 (s, 1H, CH=N). ¹³C NMR (75 MHz, DMSO-*d*₆, 25 °C): δ 10.8, 19.8, 22.6, 26.3, 29.6, 37.0, 49.8, 57.1, 62.7, 66.2, 81.5, 90.4, 119.8, 119.9, 120.9, 122.5, 124.6, 124.9, 125.4, 125.7, 127.4, 127.6, 128.1, 128.8, 130.6, 145.4, 148.6, 150.4, 151.0, 154.3, 173.0. ³¹P NMR (121.5 MHz, DMSO-*d*₆, 25 °C): δ 3.79 [s, -P(O)(OPh)NH]. C₄₀H₃₉BrClN₆O₆P (846.12): HRMS: calcd. (MW+H) 845.1613; found 845.1604.

Compound 7cB. 62 mg (26%), mp 98 °C (dec.) from EtOH/H₂O. IR: ν 3701 (NH), 1750 (C=O), 1641 (C=N) cm⁻¹. ¹H NMR (300 MHz, DMSO-*d*₆, 25 °C): δ 0.75 (t, 3H, *J* 7 Hz, CH₃), 1.16 (m, 4H+3H, CH₃ and CH₂), 1.25 (m, 1H, CH), 2.80 and 3.02 (m, 1H+1H, CH₂), 3.85 (m, 2H, CH₂-O), 4.79 (bs, 1H, CH-N), 5.04 (m, 1H, H4_{isox.}), 5.55 (bs, 1H, CH-O), 5.65 (m, 1H, H5_{isox.}), 6.30 (m, 1H, NH), 7.00 (m, 3H, arom.), 7.67 (m, 6H, arom.), 8.10 (m, 1H, CH=N), 8.13 (m, 3H, arom.), 8.53 (m, 2H, arom.), 8.58 (s, 1H, CH=N), 8.82 (m, 2H, arom.). ¹³C NMR (75 MHz, DMSO-*d*₆, 25 °C): δ 10.7, 19.1, 22.4, 26.2, 30.7, 37.5, 49.2, 61.5, 65.5, 65.8, 79.5, 88.9, 119.2, 119.3, 120.0, 124.1, 124.6, 125.0, 125.5, 125.7, 127.7, 128.1, 128.9, 129.0, 129.4, 145.4, 146.1, 151.5, 151.9, 154.1, 172.4. ³¹P NMR (121.5 MHz, DMSO-*d*₆, 25 °C): δ 2.90 [s, -P(O)(OPh)NH]. C₄₀H₃₉BrClN₆O₆P (846.12): HRMS: calcd. (MW+H) 845.1613; found 845.1593.

Acknowledgements

Financial support by the University of Pavia is gratefully acknowledged. We thank the project “Scent of Lombardy” (CUP: E31B19000700007) for financial support. PQ thanks the Hawler Medical University, Erbil, Kurdistan Region (Iraq) for granting SMA and financial support.

References

1. Gilad, Y.; Senderowitz, H. *J. Chem. Inf. Model.* **2014**, *54*, 96.
<https://doi.org/10.1021/ci400352t>
2. Mukae, M.; Ihara, T.; Tabara, M.; Jyo, A. *Org. Biomol. Chem.* **2009**, *7*, 1349.
<https://doi.org/10.1039/b821869b>
3. Ahmed, S. M.; Hussain, F. H. S.; Quadrelli, P. *Monatsh. Chem.* **2020**, *151*, 1643.
<https://doi.org/10.1007/s00706-020-02695-2>
4. Rescifina, A.; Chiacchio, U.; Corsaro, A.; Piperno, A.; Romeo, R. *Eur. J. Med. Chem.* **2011**, *46*, 129.
<https://doi.org/10.1016/j.ejmech.2010.10.023>
5. Rescifina, A.; Chiacchio, U.; Piperno, A.; Sortino, S. *New J. Chem.* **2006**, *30*, 554.
<https://doi.org/10.1039/b517150d>
6. Quadrelli, P. in *Modern Applications of Cycloaddition Chemistry*, Elsevier: Amsterdam: 2019, pp 1-152.
<https://doi.org/10.1016/B978-0-12-815273-7.00001-0>
7. Memeo, M. G.; Lapolla, F.; Maga, G.; Quadrelli, P. *Tetrahedron Lett.* **2015**, *56*, 1986 and references therein.
<https://doi.org/10.1016/j.tetlet.2015.02.114>
8. Rai, S.; Kasturi, C.; Grayzar, J.; Platz, M. S.; Goodrich, R. P.; Yerram, N. R.; Wong, V.; Tay-Goodrich, B. H. *Photochem. Photobiol.* **1993**, *58*, 59.
<https://doi.org/10.1111/j.1751-1097.1993.tb04904.x>
9. Moggio, Y.; Legnani, L.; Bovio, B.; Memeo, M. G.; Quadrelli, P. *Tetrahedron* **2012**, *68*, 1384.
<https://doi.org/10.1016/j.tet.2011.12.047>
10. Zhang, Y.; Jiao, Z.; Xu, W.; Fu, Y.; Zhu, D.; Xu, J.; He, Q.; Cao, H.; Cheng, J. *New J. Chem.* **2017**, *41*, 3790.
<https://doi.org/10.1039/C7NJ00851A>
11. Memeo, M. G.; Quadrelli, P. *Chem. Rev.* **2017**, *117*, 2108.
<https://doi.org/10.1021/acs.chemrev.6b00684>
12. Quadrelli, P.; Scrocchi, R.; Caramella, P.; Rescifina, A.; Piperno, A. *Tetrahedron* **2004**, *60*, 3643.
<https://doi.org/10.1016/j.tet.2004.02.057>
13. Ishikura, M.; Murakami, A.; Katagiri, N. *Org. Biomol. Chem.*, **2003**, *1*, 452.

- <https://doi.org/10.1039/b210963h>
14. Oliveira, F. M.; Barbosa, L. C. A.; Ismail, F. M. D. *RSC Adv.* **2014**, 4, 18998.
<https://doi.org/10.1039/C4RA01454E>
15. Yoshikawa, M.; Kato, T.; Takenishi, T. *Bull. Chem. Soc. Jpn.* **1969**, 42, 3505.
<https://doi.org/10.1246/bcsj.42.3505>
16. Caton-Williams, J.; Lin, L.; Smith, M.; Huang, Z. *Chem. Commun.* **2011**, 47, 8142.
<https://doi.org/10.1039/c1cc12201k>
17. Siegel, D.; Hui, H. C.; Doerffler, E.; Clarke, M. O.; Chun, K.; Zhang, L.; Neville, S.; Carra, E.; Lew, W.; Ross, B.; Wang, Q.; Wolfe, L.; Jordan, R.; Soloveva, V.; Knox, J.; Perry, J.; Perron, M.; Stray, K. M.; Barauskas, O.; Feng, J. Y.; Xu, Y.; Lee, G.; Rheingold, A. L.; Ray, A. S.; Bannister, R.; Strickley, R.; Swaminathan, S.; Lee, W. A.; Bavari, S.; Cihlar, T.; Lo, M. K.; Warren, T. K.; Mackman, R. L. *J. Med. Chem.* **2017**, 60, 1648.
<https://doi.org/10.1021/acs.jmedchem.6b01594>
18. Al Bujuq, N. *Synthesis* **2020**, 52, 3735.
<https://doi.org/10.1055/s-0040-1707386>
19. S. Berger, S. Braun, H.-O. Kalinowski "NMR Spectroscopy of the Non-Metallic Elements" John Wiley & Sons, Eds. 1997.
20. Cannalire, R.; Cerchia, C.; Beccari, A. R.; Di Leva, F. S.; Summa, V. *J. Med. Chem.* **2020**,
<https://doi.org/10.1021/acs.jmedchem.0c01140>
21. Gaussian 09, Revision A.02, M. J. Frisch, G. W. Trucks, H. B. Schlegel, G. E. Scuseria, M. A. Robb, J. R. Cheeseman, G. Scalmani, V. Barone, G. A. Petersson, H. Nakatsuji, X. Li, M. Caricato, A. Marenich, J. Bloino, B. G. Janesko, R. Gomperts, B. Mennucci, H. P. Hratchian, J. V. Ortiz, A. F. Izmaylov, J. L. Sonnenberg, D. Williams-Young, F. Ding, F. Lipparini, F. Egidi, J. Goings, B. Peng, A. Petrone, T. Henderson, D. Ranasinghe, V. G. Zakrzewski, J. Gao, N. Rega, G. Zheng, W. Liang, M. Hada, M. Ehara, K. Toyota, R. Fukuda, J. Hasegawa, M. Ishida, T. Nakajima, Y. Honda, O. Kitao, H. Nakai, T. Vreven, K. Throssell, J. A. Montgomery, Jr., J. E. Peralta, F. Ogliaro, M. Bearpark, J. J. Heyd, E. Brothers, K. N. Kudin, V. N. Staroverov, T. Keith, R. Kobayashi, J. Normand, K. Raghavachari, A. Rendell, J. C. Burant, S. S. Iyengar, J. Tomasi, M. Cossi, J. M. Millam, M. Klene, C. Adamo, R. Cammi, J. W. Ochterski, R. L. Martin, K. Morokuma, O. Farkas, J. B. Foresman, and D. J. Fox, Gaussian, Inc., Wallingford CT, 2016.

This paper is an open access article distributed under the terms of the Creative Commons Attribution (CC BY) license (<http://creativecommons.org/licenses/by/4.0/>)